Connectivity Performance Evaluation for Grant-Free Narrowband IoT with Widely Linear Receivers

Ronghua Gui, Naveen Mysore Balasubramanya, Lutz Lampe

Abstract—**Future wireless cellular communication networks are expected to provide connectivity for massive machine-type communication (mMTC) devices. The main challenge of supporting mMTC traffic for a cellular network lies in the high density of these devices, which individually have relatively little data to transmit. This suggests the use of a low-overhead, grant-free access scheme for uplink data transmission, which however suffers from packet collisions when devices attempt to access the channel. In this paper, we suggest the use of real-valued transmission together with widely linear (WL) reception for improving resource access and thus data throughput in the uplink of mMTC traffic scenarios. We show that, not surprisingly, the WL scheme can virtually double the number of receive antennas at the base station (BS). We analyze the effect of this on the supported user density and data throughput for grant-free uplink transmission. As a specific example, we consider the narrowband Internet-of-things (NB-IoT) cellular communication system, which already includes real-valued modulation modes. Our numerical results show that the supported user density and data throughput of grant-free NB-IoT systems can be significantly improved due to the use of WL receivers. For example, considering an NB-IoT system with 1% packet drop probability, we obtain a ten-fold (for single-antenna BS) and a six-fold (for dual-antenna BS) increase in the supported user density by using WL receivers instead of their CL counterparts.**

Index Terms—**Machine-type communication (MTC), massive connectivity, narrowband Internet-of-things (NB-IoT), widely linear (WL) receiver, user density analysis.**

I. INTRODUCTION

One critical challenge for future wireless cellular communication networks is to provide connectivity for machine-type communication (MTC) devices, such as smart utility meters, sensors for object, traffic or environmental monitoring, and inventory tracking systems [2]. Driven by the proliferation of these Internet-of-things (IoT) applications, MTC devices are expected to accumulate massively in the near future, leading to massive MTC (mMTC) scenarios [3].

Current solutions to enable massive connectivity mainly fall into two categories: medium access control (MAC) and physical (PHY) layer solutions [4]. The MAC-layer solutions aim to re-design the access protocols such that the limited time-frequency resource can be shared by more devices. For example, as a new third generation partnership project (3GPP) technology toward mMTC scenarios, the narrowband IoT (NB-IoT) standard [5], [6] enables subcarrier-level resource allocation and supports single-tone transmissions with a subcarrier spacing as low as 3.75 kHz, which allows more devices

to be served simultaneously. Another example is the grant-free transmission [7], which is largely simplified compared to the multi-stage access control protocols in legacy long-term evolution (LTE) networks. Consequently, the control signalling overhead can be remarkably reduced, which is critical for small-size data packets typical for IoT applications. On the other hand, the PHY-layer solutions are mostly based on advanced receiver techniques, including successive interference cancellation (SIC)-based and compressive-sensing (CS)-based multi-user[1] detection. SIC arises in power-domain non-orthogonal multi-access (NOMA) [8], where the multiple signals with power differences can be decoded successively. CS-based methods have frequently been applied to user activity detection for sporadic traffic [9] and data decoding with sparse codebooks [10]. Both SIC and CS methods are applicable for data decoding in the signature-based NOMA (S-NOMA) schemes [11], where the signature represents the way the data stream of an active device is spread over available resources, e.g., device-specific codebook structures, delay patterns and spreading sequences etc., in a non-orthogonal manner.

In this paper, we consider the use of widely linear (WL) processing to further aid the support of massive connectivity in mMTC networks. WL processing differs from conventional linear (CL) processing in that the former processes not only the received signal, but also its complex conjugate [12]. It has been shown that the user-multiplexing capability of linear multi-user receivers can be significantly enhanced by WL processing [13]–[15]. This requires that users employ signal constellations that can be interpreted as one-dimensional at the receiver [16], such as pulse-amplitude modulation (PAM) or Gaussian minimum-shift keying (GMSK). Hence, WL receivers, i.e., linear-type multi-user receivers combined with WL processing, are a promising PHY-layer solution for massive connectivity.

A. WL Processing for Communications

Data communication signals are often assumed to satisfy the condition of second-order circularity [17], in which case, CL processing based on the usual covariance matrix is linearly optimal [18]. However, when the communication signals become second-order non-circular, e.g., in the case of real-valued data sequences generated by one-dimensional constellations, CL processing is unable to exploit the complete second-order statistic. Hence, WL processing, initially proposed to

---

[1] We will use the terms "user" and "device" synonymously for terminals participating in the cellular MTC. The former has commonly been used for signal-processing methods for cellular communication such as multi-user detection, while the latter is more closely linked to the MTC-for-IoT scenario considered in this paper.

deal with the second-order non-circularity [12], has been shown to outperform CL processing. Examples for this include the cancellation of co-channel interference in GMSK-based cellular communication networks [14], the suppression of multi-access interferences with real-valued constellations in direct-sequence code-division multiple-access (DS-CDMA) [16] and in multi-antenna systems [19], [20], adaptive array beamforming for noncircular signals [15], and the mitigation of in-phase/quadrature (IQ) imbalances [21].

B. Motivation

In this paper, we investigate the application of WL receivers[2] for the uplink of mMTC transmission scenarios with the objective of increasing the admissible IoT-device density or equivalently the system throughput for a given density. WL processing has also been considered for MIMO systems with real-valued transmissions, network-assisted interference cancellation in LTE [22] and inter-symbol interference mitigation in enhanced mobile broadband (eMBB) uplink transmission assuming real-valued (one-dimensional) modulation [23]. However, the application of WL processing for further enhancing the connectivity capability of mMTC networks has not been reported so far.

One prominent cellular solution that supports mMTC is the NB-IoT technology [24], [25]. NB-IoT has been designed to coexist with legacy LTE networks and to provide extended coverage, massive connectivity, and low cost and power implementations suitable for IoT [5], [6]. For example, NB-IoT has been reported to support a coverage of up to 8 km for urban areas, up to 50k devices per cell site sector (0.86 km^2), with a battery life of up to 10 years and at a cost of no more than \$5 per device [26]. Interestingly, the NB-IoT uplink permits one-dimensional transmission using $\frac{\pi}{2}$-binary phase-shift keying (BPSK)[3], which simplifies the NB-IoT user equipment (UE) design, assists in coverage enhancement and is sufficient to support the data rate requirements in the uplink. Considering the application of NB-IoT to mMTC scenarios, it is desirable to design mechanisms that can further improve the performance of NB-IoT networks, especially in terms of the number of devices supported per sector. Prior works in NB-IoT do not explore the use of WL processing to increase the supported user density. Also, past works in WL do not provide an analysis of the outage probability, which is a key performance indicator in wireless communication networks.

C. Contributions

To the best of our knowledge, our previous work in [1] was the first attempt to exploit the one-dimensional modulation using WL processing to enhance the supported user density

of an NB-IoT system and present the outage probability analysis for such a system. However, it only considered a single-antenna receiver at the BS. In this journal extension, we present the analysis for the general case of multi-antenna WL receivers with both zero-forcing (WL-ZF) and minimum mean squared error (WL-MMSE) processing. We consider grant-free uplink transmission protocol, which is generally accepted as one of the most suitable MAC layer solutions for massive connectivity [4], [7], [9], [10], [27] and is also being considered for standardization in Release 16 of NB-IoT. The main contributions of this paper are as follows.

- We show that, employing our WL transform introduced in [1] renders the outage probability analysis of WL-ZF and WL-MMSE for the multi-antenna case to be similar to that of their CL counterparts in MIMO scenarios. This enables us to present analytical expressions for the outage probability of the WL-ZF receiver and an asymptotic analysis of the same for WL-MMSE receivers in the high SNR regime. Results indicate that our theoretical analysis for WL-ZF and the asymptotic analysis for WL-MMSE match very well with the numerical results obtained from simulations.
- Based on the outage probability expressions, we show that the WL receivers are superior to their CL counterparts in terms of user-multiplexing capability and transmission reliability. In particular, we apply the outage probability results for the connectivity performance evaluation of grant-free MTC networks using WL receivers, considering the three key performance indicators - packet drop probability, supported user density and system throughput.
- Considering a grant-free NB-IoT system for performance evaluation, we demonstrate that the WL receivers have a lower packet drop probability than their CL counterparts and thus can support higher device density and system throughput for a given packet drop probability. Specifically, for a target packet drop probability of 1% and a single-antenna BS, we illustrate that an NB-IoT BS with CL processing can support up to 50k users per sector, while that with the proposed WL processing can support up to 500k users per sector, which is a ten-fold increase. We show that WL processing provides a more than three-fold gain in the number of supported users for the same target packet drop probability even when the number of BS antennas is increased to four, which further justifies the advantage of our proposed method.

Our WL-ZF and WL-MMSE receivers not only increase the supported user density, but also provide a mechanism which can be employed in an NB-IoT BS with minimal changes to its signal processing chain.

D. Organization

The rest of this paper is organized as follows. The signal model for real-valued transmission and WL reception is presented in Section II. The outage performance of WL-ZF and WL-MMSE receivers is analyzed in Section III. Then the outage probability results are used to evaluate the connectivity

---

[2]The use of WL receivers is meaningful in the case of one-dimensional (or real-valued) modulation. For brevity, we omit the explicit mention of this in the following, i.e., when referring to WL receivers or detection, the real-valued modulation is implied. Similarly, when referring to CL receivers or detection, complex-valued modulation is assumed.

[3]In the NB-IoT specification, $\frac{\pi}{2}$-BPSK modulation has been adopted to reduce the peak-to-average power ratio compared to BPSK. As far as the applicability of WL receivers is concerned, there is no difference between BPSK and $\frac{\pi}{2}$-BPSK, as both are one-dimensional modulations.

performance of MTC systems using WL receivers in Section IV. Numerical results for NB-IoT system parameters are presented and discussed in Section V, followed by conclusions in Section VI.

II. Signal Model for Widely Linear Reception

We consider cellular uplink transmission scenario in which the base station (BS) is located in the cell centre and provides connectivity for a large number of spatially uniformly deployed single-antenna users. Upon a data packet arrival, following the grant-free access strategy, each user selects randomly one of the subsequent time-frequency resource blocks (TFRB). In the context of NB-IoT systems, a TFRB consists of one or several sub-carriers and lasts during the transmission time interval (TTI). All transmissions are assumed to be synchronized at TTI level.

A. Multi-User Model

Assuming further, without loss of generality, that there are N active single-carrier transmission users occupying the same TFRB, the complex baseband signal received at the M-antenna BS for this TFRB can be expressed as

$$\bar{y} = \sum_{i=1}^{N} \sqrt{p_{\mathrm{T,av}}} \bar{g}_i s_i + \bar{n}, \tag{1}$$

where $\bar{y} \in \mathbb{C}^{M \times 1}$ is the vector of complex received samples, and $p_{\mathrm{T,av}} \triangleq \mathbb{E}\{p_{\mathrm{T},i}\}$ denotes the average transmit power, with $\mathbb{E}\{\cdot\}$ and $p_{\mathrm{T},i}$ representing the statistical expectation and the instantaneous transmit power for the ith user, respectively. The message for the ith user, generated from a real-valued modulation scheme, is denoted by $s_i \in \mathbb{R}$, $1 \leq i \leq N$. The considered signal constellations are zero mean and normalized according to $\mathbb{E}\{|s_i|^2\} = 1$, and signals from different users are statistically independent. The complex channel gain vector $\bar{g}_i \in \mathbb{C}^{M \times 1}$ is modelled as

$$\bar{g}_i = \sqrt{\phi_i} \bar{h}_i \tag{2}$$

where the channel vector $\bar{h}_i \in \mathbb{C}^{M \times 1}$, accounting for small-scale fading, consists of independently and identically distributed (i.i.d.) complex Gaussian components, i.e., $\bar{h}_i \sim \mathcal{CN}(0, I_M)$, with I_M denoting the $M \times M$ identity matrix. The term ϕ_i represents the received power variation due to power control and large-scale fading, and is expressed as

$$\phi_i \triangleq \frac{p_{\mathrm{T},i} \beta_i \psi_i}{p_{\mathrm{T,av}}} \tag{3}$$

where β_i and ψ_i denote the pathloss and shadowing fading factors, respectively. Through specifying $p_{\mathrm{T},i}$, β_i and ψ_i with different distributions, the power variation term ϕ_i is expected to model the power control and large-scale fading process in many applications, e.g., the case of no power control (NPC) can be modelled with $p_{\mathrm{T},i} = p_{\mathrm{T}}, \forall i$, and perfect power compensation (PPC) with $p_{\mathrm{T},i} = p_{\mathrm{T,av}} \frac{(\beta_i \psi_i)^{-1}}{\mathbb{E}\{(\beta_i \psi_i)^{-1}\}}$. In general cases, $p_{\mathrm{T},i}$ is a more complicated function of β_i and ψ_i, depending on the specific power control strategy of the target system. Herein, we do not specify any concrete distribution

for ϕ_i, but instead assume that ϕ_i, $i = 1, 2, \ldots, N$, are i.i.d. for analytical tractability. This assumption is valid for practical MTC scenarios, where all the MTC devices use an identical but independent power control process, e.g., in the case of open-loop power control of various cellular IoT systems [26]. Finally, $\bar{n} \sim \mathcal{CN}(0, \sigma_{\mathrm{c}}^2 I_M)$, where σ_{c}^2 is the complex noise variance. For convenience, we define the transmit signal-to-noise ratio (SNR) as

$$\rho \triangleq \frac{p_{\mathrm{T,av}}}{\sigma_{\mathrm{c}}^2}. \tag{4}$$

B. Widely Linear Reception

In order to make use of the prior knowledge about real-valued transmission, we apply the WL transform[4] $\mathcal{T} : \bar{x} \in \mathbb{C}^M \to x \in \mathbb{R}^{2M}$ with $x = \mathcal{T}(\bar{x}) \triangleq [\mathrm{Re}(\bar{x}^T), \mathrm{Im}(\bar{x}^T)]^T$, where $\mathrm{Re}(\cdot)$ and $\mathrm{Im}(\cdot)$ denote the real and imaginary parts, respectively, to the complex-valued vectors $\bar{y}$, $\bar{g}_i$, $\bar{h}_i$, and $\bar{n}$ defined above. Then, $h_i \sim \mathcal{N}(0, I_{2M}/2)$ and $n \sim \mathcal{N}(0, \sigma_{\mathrm{c}}^2 I_{2M}/2)$, and we can rewrite the signal model (1) as

$$y = \sum_{i=1}^{N} \sqrt{p_{\mathrm{T,av}}} g_i s_i + n. \tag{5}$$

After the WL transform, since the users employ one-dimensional modulation schemes, a complex-valued signal will actually contain the superposition of two user signals. Therefore, the BS with M receiver antennas using WL processing can serve $2M$ users. In other words, the number of BS antennas has been virtually doubled. We assume that the number of active users per TFRB satisfies $N \leq 2M$, and that the channel state information can be perfectly tracked by the BS receiver, i.e., g_i for $1 \leq n \leq N$ are known at the receiver. This permits the use of linear interference suppression via applying a vector $u_n \in \mathbb{R}^{2M}$ to the WL transformed signal y from (5) for the detection of the message s_n, $1 \leq n \leq N$. Hence, the decision variable for WL detection for the nth user signal can be written as

$$r_n = u_n^T y$$
$$= \sqrt{p_{\mathrm{T,av}}} u_n^T g_n s_n + \sum_{i=1, i \neq n}^{N} \sqrt{p_{\mathrm{T,av}}} u_n^T g_i s_i + u_n^T n. \tag{6}$$

where $(\cdot)^T$ denotes the transpose. The resulting output signal-to-interference-plus-noise ratio (SINR) for the nth user is given by

$$\gamma_n = \frac{p_{\mathrm{T,av}} |u_n^T g_n|^2}{p_{\mathrm{T,av}} \sum_{i=1, i \neq n}^{N} |u_n^T g_i|^2 + \frac{1}{2} \sigma_{\mathrm{c}}^2 \|u_n\|^2}. \tag{7}$$

where $\|\cdot\|$ denotes the ℓ_2 norm.

---

[4]The WL transform used in literature typically employs the complex-valued signal and its complex conjugate transpose [12], [15], [16], [18], [19], [21]. However, the WL transform that we employ stacks the real and imaginary parts of the complex signal separately. Such a transformation not only makes it more convenient to handle two different users using one-dimensional modulation, but also renders the analysis to be similar to that used for MIMO schemes, e.g. [28], [29]. In particular, the analysis is similar to that of a MIMO system with $2M$ receiver antennas.

In analogy to the CL-ZF and CL-MMSE multi-user detectors [29], we can derive the WL-ZF and WL-MMSE receivers for detecting the nth user as

$$\boldsymbol{u}_n = \begin{cases} \boldsymbol{G}_{\bar{n}}^{\perp} \boldsymbol{g}_n & \text{for WL ZF} \\ \boldsymbol{R}_{\bar{n}}^{-1} \boldsymbol{g}_n & \text{for WL MMSE} \end{cases} \quad (8)$$

where

$$\boldsymbol{G}_{\bar{n}}^{\perp} \triangleq \boldsymbol{I}_{2M} - \boldsymbol{G}_{\bar{n}} \left[\boldsymbol{G}_{\bar{n}}^T \boldsymbol{G}_{\bar{n}} \right]^{-1} \boldsymbol{G}_{\bar{n}}^T \quad (9)$$

is the orthogonal projecting matrix of the interference channel matrix

$$\boldsymbol{G}_{\bar{n}} \triangleq \begin{bmatrix} \boldsymbol{g}_1 & \cdots & \boldsymbol{g}_{n-1} & \boldsymbol{g}_{n+1} & \cdots & \boldsymbol{g}_N \end{bmatrix} , \quad (10)$$

and

$$\boldsymbol{R}_{\bar{n}} = 2\rho \boldsymbol{G}_{\bar{n}} \boldsymbol{G}_{\bar{n}}^T + \boldsymbol{I}_{2M} \quad (11)$$

is the interference-plus-noise covariance matrix. Inserting (8) into (7) yields the output SINRs for the WL-ZF and WL-MMSE detectors for the nth user signal as

$$\gamma_{\text{WZF},n} = 2\rho \phi_n \boldsymbol{h}_n^T \boldsymbol{G}_{\bar{n}}^{\perp} \boldsymbol{h}_n \quad (12a)$$

$$\gamma_{\text{WMMSE},n} = 2\rho \phi_n \boldsymbol{h}_n^T \boldsymbol{R}_{\bar{n}}^{-1} \boldsymbol{h}_n . \quad (12b)$$

C. Comparison to CL Reception

1) Detector Expressions: One can apply the ZF and MMSE detection to the original complex-valued model (1) for decoding the nth user data stream, regardless of whether s_n, $1 \le n \le N$, are real-valued or not. Then, one can obtain the CL-ZF and CL-MMSE detection vectors as [29]

$$\bar{\boldsymbol{u}}_n = \begin{cases} \bar{\boldsymbol{G}}_{\bar{n}}^{\perp} \bar{\boldsymbol{g}}_n & \text{for CL ZF} \\ \bar{\boldsymbol{R}}_{\bar{n}}^{-1} \bar{\boldsymbol{g}}_n & \text{for CL MMSE} \end{cases} , \quad (13)$$

where

$$\bar{\boldsymbol{G}}_{\bar{n}}^{\perp} = \boldsymbol{I}_M - \bar{\boldsymbol{G}}_{\bar{n}} \left[\bar{\boldsymbol{G}}_{\bar{n}}^H \bar{\boldsymbol{G}}_{\bar{n}} \right]^{-1} \bar{\boldsymbol{G}}_{\bar{n}}^H \quad (14a)$$

$$\bar{\boldsymbol{R}}_{\bar{n}} = \rho \bar{\boldsymbol{G}}_{\bar{n}} \bar{\boldsymbol{G}}_{\bar{n}}^H + \boldsymbol{I}_M \quad (14b)$$

with $\bar{\boldsymbol{G}}_{\bar{n}} = \begin{bmatrix} \bar{\boldsymbol{g}}_1 & \cdots & \bar{\boldsymbol{g}}_{n-1} & \bar{\boldsymbol{g}}_{n+1} & \cdots & \bar{\boldsymbol{g}}_N \end{bmatrix}$ being the channel gain matrix of the remaining $N - 1$ users, and $(\cdot)^H$ the conjugate transpose.

It is clear that the WL detection vector $\boldsymbol{u}_n$ has a similar expression as its CL counterpart $\bar{\boldsymbol{u}}_n$. The main difference lies with whether the signal model (1) has been WL-transformed or not, or equivalently, whether the prior knowledge about real-valued transmission has been utilized or not. As the CL receivers ignore the real-valued transmission, the number of supported users would be limited to M, i.e., there is no increase compared to that in the case of complex-valued transmission.

2) Implementation Complexity: The implementation of WL receivers at the BS in NB-IoT is similar to that of CL receivers. Both types of receivers require channel estimation of the user signals. The NB-IoT frame structure facilitates users to transmit pilot sequences periodically in the uplink, which are used for channel estimation by the BS. Moreover, the BS already has prior knowledge about the use of real-valued transmission, since NB-IoT scheduling mandates that the modulation scheme to be employed by a user equipment is

decided by the BS in grant-based scenarios. Data transmission size and modulation schemes are also known to the BS a priori in grant-free scenarios. Therefore, there is no additional signalling overhead required to implement the WL reception in NB-IoT systems.

In terms of the computational complexity, we analyze the WL-MMSE detector in (8) as an example. The computation of $\boldsymbol{G}_{\bar{n}} \boldsymbol{G}_{\bar{n}}^T$ and the inversion of $\boldsymbol{R}_{\bar{n}}$ require $\mathcal{O}\left(4M^2N\right)$ and $\mathcal{O}\left(8M^3\right)$ multiplications, respectively. The computational complexity of product $\boldsymbol{R}_{\bar{n}}^{-1} \boldsymbol{g}_n$ is $\mathcal{O}\left(4M^2\right)$. Hence, the total number of multiplications for obtaining the WL-MMSE detector is $\mathcal{O}\left(4M^2N\right) + \mathcal{O}\left(8M^3\right) + \mathcal{O}\left(4M^2\right) = \mathcal{O}\left(M^3\right)$, where $N \le 2M$ has been used. Similarly, the number of multiplications required to compute the WL-ZF detector is $\mathcal{O}\left(M^2N\right)$. The numbers of multiplications for computing the CL-MMSE and CL-ZF detectors are $\mathcal{O}\left(M^2N + M^3\right)$ and $\mathcal{O}\left(MN^2 + N^3 + M^2N\right)$, respectively. As the number of supported users is $N \le M$ for CL detection, the computational complexities of CL-ZF and CL-MMSE receivers reduce to $\mathcal{O}\left(M^2N\right)$ and $\mathcal{O}\left(M^3\right)$ in the case of $N \le M$. Consequently, the WL and CL receivers have approximately the same computational complexity when they decode the same number of user streams. Furthermore, approaches avoiding explicit matrix inversion to implement approximate MMSE filters, see e.g. [30], are equally applicable to WL and CL receivers.

III. OUTAGE PROBABILITY OF WIDELY LINEAR RECEIVERS

In this section, we derive analytical expressions for the outage probability of WL receivers according to the system model introduced above. The outage probability is a measure for the block or packet error rate for coded transmission, without making specific assumptions on the error-correction coding format or decoding algorithm and block length. We note that the outage probability of WL receivers has not been analyzed in previous work such as [19], [20], which only considered the uncoded error probability, i.e., symbol error rate. For analytical tractability, we make the common assumption that the interference can be treated as Gaussian distributed. Then the outage probability of WL receivers for simultaneously decoding N user data streams is given by

$$\mathcal{P}_{\text{WL}}(N) = \Pr\left(\frac{1}{2} \log\left(1 + \frac{\gamma_{\text{WL}}}{\Gamma} \right) \le R \right), \quad (15)$$

where the factor $1/2$ is due to the real-valued transmission [29], γ_{WL} is the output SINR of the respective WL receiver in (12), $\Gamma > 1$ is the SNR gap to account for the performance loss of a practical coding and modulation schemes with respect to the channel capacity, and R is the target data rate in bit per channel use, i.e., bits/sec/Hz assuming idealized band-limited pulse-shapes.

A. WL-ZF Receiver

First, we consider the WL-ZF receiver. Let $\boldsymbol{G}_{\bar{n}}^{\perp} = \boldsymbol{Q}_{\bar{n}}^T \boldsymbol{\Lambda} \boldsymbol{Q}_{\bar{n}}$ be the eigenvalue decomposition of $\boldsymbol{G}_{\bar{n}}^{\perp}$, where $\boldsymbol{Q}_{\bar{n}} \in \mathbb{R}^{2M \times 2M}$ is an orthogonal matrix satisfying $\boldsymbol{Q}_{\bar{n}}^T \boldsymbol{Q}_{\bar{n}} = \boldsymbol{Q}_{\bar{n}} \boldsymbol{Q}_{\bar{n}}^T = \boldsymbol{I}_{2M}$ and $\boldsymbol{\Lambda} = \text{diag}\{\lambda_1, \lambda_2, ..., \lambda_{2M}\}$ is a diagonal

matrix, where $\lambda_1 \geq \lambda_2 \geq \cdots \geq \lambda_{2M}$ are the ordered eigenvalues of $G_{\bar{n}}^{\perp}$. Since $G_{\bar{n}}^{\perp}$ is the orthogonal projecting matrix, which projects vectors to the subspace orthogonal to the range of $G_{\bar{n}}$, its eigenvalues are either 1 or 0 [31]. As the column space of $G_{\bar{n}}$ has dimension $N-1$, the dimension of its orthogonal subspace equals to $2M - (N-1)$. Thus, the first $2M - (N-1)$ eigenvalues are ones and the remaining are zeros, i.e.,

$$\Lambda = \begin{bmatrix} I_{2M-N+1} & 0 \\ 0 & 0 \end{bmatrix}. \tag{16}$$

Using the eigenvalue decomposition, we can expand the output SINR of the WL-ZF receiver (12a) as

$$\gamma_{\mathrm{WZF},n} = 2\rho\phi_n h_n^T Q_{\bar{n}}^T \Lambda Q_{\bar{n}} h_n = \rho\phi_n \sum_{i=1}^{2M-N+1} \left[\sqrt{2} Q_{\bar{n}} h_n \right]_i^2, \tag{17}$$

where $\left[\sqrt{2} Q_{\bar{n}} h_n \right]_i$ is the ith entry of vector $\sqrt{2} Q_{\bar{n}} h_n$ and $\left[\sqrt{2} Q_{\bar{n}} h_n \right]_i \sim \mathcal{N}(0,1)$. Hence, it follows that

$$\frac{\gamma_{\mathrm{WZF},n}}{\rho\phi_n} \sim \chi_{2M-N+1}^2, \tag{18}$$

where χ_{2M-N+1}^2 stands for the standard Chi-squared distribution with $2M - N + 1$ degrees of freedom (DoFs).

Applying (18) to (15), we calculate the outage probability of the WL-ZF receiver for the nth user as

$$\begin{aligned} \mathcal{P}_{\mathrm{WZF}}(N) &= \Pr\left(\frac{1}{2} \log\left(1 + \frac{\gamma_{\mathrm{WZF},n}}{\Gamma} \right) \leq R \right) \\ &= \Pr\left(\frac{\gamma_{\mathrm{WZF},n}}{\rho\phi_n} \leq \frac{\Gamma \left(2^{2R} - 1 \right)}{\rho\phi_n} \right) \\ &= \int_0^{\infty} F_{\chi_{2M-N+1}^2}\left(\frac{\Gamma\gamma_R}{\rho x} \right) f_\phi(x)\,\mathrm{d}x, \end{aligned} \tag{19}$$

where $F_{\chi_{2M-N+1}^2}(x)$ denotes the cumulative distribution function (CDF) of the standard Chi-squared distribution χ_{2M-N+1}^2, $\gamma_R = 2^{2R} - 1$ denotes the target SINR and $f_\phi(x)$ denotes the probability density function (PDF) of ϕ_n. Note that $\mathcal{P}_{\mathrm{WZF}}(N)$ is the same for all users as we assumed identical distributions for combined pathloss and small-scale fading.

B. WL-MMSE Receiver

For the WL-MMSE receiver, we follow the analysis in [28] for the CL-MMSE receiver and decompose the output SINR $\gamma_{\mathrm{WMMSE},n}$ into the sum of $\gamma_{\mathrm{WZF},n}$ and an additional term $\gamma_{\Delta,n}$:

$$\gamma_{\mathrm{WMMSE},n} = \gamma_{\mathrm{WZF},n} + \gamma_{\Delta,n}, \tag{20}$$

where the SINR difference term can be calculated as

$$\gamma_{\Delta,n} = 2\rho\phi_n h_n^T \left(R_{\bar{n}}^{-1} - G_{\bar{n}}^{\perp} \right) h_n. \tag{21}$$

Inserting (9) and (11) into (21) and using the matrix inversion lemma, we obtain

$$\gamma_{\Delta,n} = 2\rho\phi_n h_n^T \Pi_{\bar{n}} h_n, \tag{22}$$

where

$$\Pi_{\bar{n}} = G_{\bar{n}} \left(G_{\bar{n}}^T G_{\bar{n}} \right)^{-1} G_{\bar{n}}^T - G_{\bar{n}} \left(G_{\bar{n}}^T G_{\bar{n}} + \frac{1}{2\rho} I_{2M} \right)^{-1} G_{\bar{n}}^T. \tag{23}$$

In order to further simplify (23), we consider the high SNR regime, i.e., $\rho \to \infty$, for which the approximation

$$\begin{aligned} &\left(G_{\bar{n}}^T G_{\bar{n}} + \frac{1}{2\rho} I_{2M} \right)^{-1} \\ &\approx \left(G_{\bar{n}}^T G_{\bar{n}} \right)^{-1} - \frac{1}{2\rho} \left(G_{\bar{n}}^T G_{\bar{n}} \right)^{-1} \left(G_{\bar{n}}^T G_{\bar{n}} \right)^{-1} \end{aligned} \tag{24}$$

is tight. Using (24) in (23), after simple manipulations, allows us to write (20) as

$$\frac{\gamma_{\mathrm{WMMSE},n}}{\phi_n} \simeq \frac{\gamma_{\mathrm{WZF},n}}{\phi_n} + \eta_{\mathrm{WL},n}, \tag{25}$$

where $\simeq$ represents the asymptotic equality in the high SNR regime and $\eta_{\mathrm{WL},n} \triangleq \gamma_{\Delta,n}/\phi_n$ is given by

$$\eta_{\mathrm{WL},n} = h_n^T H_{\bar{n}} \left(H_{\bar{n}}^T H_{\bar{n}} \right)^{-1} \Phi_{\bar{n}}^{-1} \left(H_{\bar{n}}^T H_{\bar{n}} \right)^{-1} H_{\bar{n}}^T h_n, \tag{26}$$

with

$$H_{\bar{n}} \triangleq [h_1, ..., h_{n-1}, h_{n+1}, .., h_N] \tag{27}$$

$$\Phi_{\bar{n}} \triangleq \mathrm{diag}\left\{ \phi_1, ..., \phi_{n-1}, \phi_{n+1}, .., \phi_N \right\}. \tag{28}$$

Applying the same argument as in [28] for the CL-MMSE receiver, it follows that $\eta_{\mathrm{WL},n}$ is independent of $\gamma_{\mathrm{WZF},n}/\phi_n$. Hence, using (25), we obtain a fairly compact expression for the outage probability of the WL-MMSE receiver in the high SNR regime as

$$\begin{aligned} \mathcal{P}_{\mathrm{WMMSE}}(N) &= \Pr\left(\frac{1}{2} \log\left(1 + \frac{\gamma_{\mathrm{WMMSE},n}}{\Gamma} \right) \leq R \right) \\ &\simeq \Pr\left(\frac{\gamma_{\mathrm{WZF},n}}{\rho\phi_n} + \frac{\eta_{\mathrm{WL},n}}{\rho} \leq \frac{\Gamma \left(2^{2R} - 1 \right)}{\rho\phi_n} \right) \\ &= \int_0^{\infty} \int_0^{\frac{\Gamma\gamma_R}{x}} F_{\chi_{2M-N+1}^2}\left(\frac{\Gamma\gamma_R}{\rho x} \left[1 - \frac{xy}{\Gamma\gamma_R} \right] \right) \\ &\quad \times f_{\eta_{\mathrm{WL}}}(y) f_\phi(x) \mathrm{d}y\,\mathrm{d}x, \end{aligned} \tag{29}$$

where $f_{\eta_{\mathrm{WL}}}(y)$, $0 \leq y \leq \infty$ is the PDF of the additional term $\eta_{\mathrm{WL},n}$.

In the high SNR regime, the WL-MMSE receiver has an improved outage performance compared to the WL-ZF receiver since $\eta_{\mathrm{WL},n} > 0$ and thus $\mathcal{P}_{\mathrm{WMMSE}}(N) < \mathcal{P}_{\mathrm{WZF}}(N)$. In high rate scenarios, i.e., as $\gamma_R \to \infty$, the expression in (29) converges to (19), and thus the outage performance of WL-ZF receiver approaches that of the WL-MMSE receiver as the rate increases.

In the low SNR regime, it is difficult to analytically characterize the outage performance of the WL-MMSE receiver due to the complicated form of $\gamma_{\Delta,n}$ in (22) and (23). Nevertheless, we will show through numerical results that the asymptotic outage probability above for the WL-MMSE receiver still matches well with the exact one in a relatively wide range of SNRs.

C. Diversity Order Analysis

It is insightful to use high-SNR expressions of the outage probability to study the diversity order afforded by the WL

receivers. For this purpose, we apply the first-order approximation

$$F_{\chi_k^2}(x) \simeq \frac{1}{(k/2)\, 2^{k/2}\Gamma_{k/2}} x^{k/2}, \tag{30}$$

of $F_{\chi_k^2}(x)$ around $x = 0$, where $\Gamma_a \triangleq \int_0^\infty e^{-t} t^{a-1} \mathrm{d}t$ is the Gamma function, and obtain for $\rho \to \infty$:

$$\mathcal{P}_{\mathrm{WZF}}(N) \simeq \frac{T_{\mathrm{WZF}}}{\rho^{M-(N-1)/2}} \tag{31}$$

$$\mathcal{P}_{\mathrm{WMMSE}}(N) \simeq \frac{T_{\mathrm{WMMSE}}}{\rho^{M-(N-1)/2}} \tag{32}$$

where T_{WZF} and T_{WMMSE} are two SNR-independent constants.

In order to obtain an outage performance that improves with SNR, the receiver diversity order needs to be positive. Hence, we observe that $N_{\mathrm{WL}} \leq 2M$ users per TFRB are supported by WL receivers, as opposed to only $N_{\mathrm{CL}} \leq M$ for CL receivers (recalling the diversity order $M - (N_{\mathrm{CL}} - 1)$ for CL receivers [29]). On the other hand, for $N_{\mathrm{WL}} < 2N_{\mathrm{CL}} - 1$, the WL receivers have a higher diversity order and thus are expected to provide an improved transmission reliability compared to the CL receivers.

D. Evaluation of Outage Probability Expressions

The expressions (19) and (29) for the (asymptotic) outage probabilities of the WL-ZF and WL-MMSE receivers include improper integrals. The possibility of their reduction into simpler expressions depends on the probabilistic model of ϕ_n. In the PPC case, $\phi_n = \frac{1}{\mathbb{E}\{(\beta_n\psi_n)^{-1}\}} \triangleq \phi_{\mathrm{PPC}}, \forall n$. For the WL-ZF receiver, we obtain

$$\mathcal{P}_{\mathrm{WZF}}(N) = F_{\chi_{2M-N+1}^2}\left(\frac{\Gamma\gamma_R}{\rho\phi_{\mathrm{PPC}}}\right). \tag{33}$$

For the WL-MMSE receiver, we can show that the additional term $\eta_{\mathrm{WL},n}$ is a scaled F-distributed random variable, following the analysis for the CL-MMSE receiver in [28], and thus

$$\mathcal{P}_{\mathrm{WMMSE}}(N) \simeq \int_0^{\frac{\Gamma\tilde{\gamma}_R}{\phi_{\mathrm{PPC}}}} F_{\chi_{2M-N+1}^2}\left(\frac{\Gamma\tilde{\gamma}_R}{\rho\phi_{\mathrm{PPC}}}\left[1 - \frac{\phi_{\mathrm{PPC}}}{\Gamma\tilde{\gamma}_R}y\right]\right) \\ \times f_{\mathcal{F}_{N-1,2M-N+2}}(y)\,\mathrm{d}y\,, \tag{34}$$

where $\tilde{\gamma}_R = \frac{2M-N+2}{N-1}\gamma_R$, and $\mathcal{F}_{N-1,2M-N+2}$ stands for the standard F-distribution with DoF parameters $d_1 = N - 1$ and $d_2 = 2M - N + 2$.

For more realistic models, there is no closed-form expression for the PDF of ϕ_n and thus evaluation of (19) and (29) requires numerical integration. Noting that it is usually easy to draw samples of ϕ_n, given its generating model, we turn to Monte Carlo (MC) integration [32] for fast computation of the integral in (19). Similarly, we can generate samples of $\eta_{\mathrm{WL},n}$ easily according to (26), which, combined with the samples of ϕ_n, can be used for computing the probabilistic integral in (29) via MC integration.

IV. CONNECTIVITY PERFORMANCE EVALUATION

In this section, we evaluate the connectivity performance for the uplink transmission of grant-free MTC networks. We first present expressions for the packet collision and packet drop probabilities, based on which we can determine the supported IoT-device density and system throughput. These expressions are then combined with the outage probability results from the previous section.

A. Collision Probability

We assume that there are N_{cell} devices served by one BS and that K_{b} TFRBs are available over each TTI in the system. Furthermore, we model the traffic at all devices as a Poisson process with an arrival rate of λ_{a} packets per TTI per device, which is sufficiently low so that the queueing delay becomes negligible and the transmit probability of each device over a given TTI is $P_{\mathrm{a}} = 1 - e^{-\lambda_{\mathrm{a}}}$.

Without loss of generality, we assume that user 1 has a packet arrival and thus intends to transmit over the next TTI. The probability that N_{a} other users also have a packet arrival over the same TTI is given by

$$P_{\mathrm{act}}(N_{\mathrm{a}}) = \binom{N_{\mathrm{cell}}-1}{N_{\mathrm{a}}} P_{\mathrm{a}}^{N_{\mathrm{a}}} (1 - P_{\mathrm{a}})^{N_{\mathrm{cell}}-N_{\mathrm{a}}-1}. \tag{35}$$

Given N_{a} active users, the probability that N_{s} of them select the same TFRB as user 1 follows as

$$P(N_{\mathrm{a}}, N_{\mathrm{s}}) = \binom{N_{\mathrm{a}}}{N_{\mathrm{s}}}\left(\frac{1}{K_{\mathrm{b}}}\right)^{N_{\mathrm{s}}}\left(1 - \frac{1}{K_{\mathrm{b}}}\right)^{N_{\mathrm{a}}-N_{\mathrm{s}}}. \tag{36}$$

Hence, the collision probability, i.e., the probability that N_{s} other users select the same TFRB as user 1, is calculated as

$$P_{\mathrm{col}}(N_{\mathrm{s}}) = \sum_{N_{\mathrm{a}}=N_{\mathrm{s}}}^{N_{\mathrm{cell}}-1} P_{\mathrm{act}}(N_{\mathrm{a}}) P(N_{\mathrm{a}}, N_{\mathrm{s}}) \tag{37}$$

for $0 \leq N_{\mathrm{s}} \leq N_{\mathrm{cell}} - 1$.

B. Packet Drop Probability

In the grant-free access scenario, once the BS station receives multiple colliding packets from various users, it first performs the user activity detection and channel estimation and then passes the results to the subsequent multi-user receiver for data decoding. The first task is enabled by preamble sequences such as Zadoff-Chu [7] or i.i.d. Gaussian sequences [9], which precede the payload. Since the preamble detection is not the focus of this paper, we use the missed detection probability $P_{\mathrm{miss}}(N_{\mathrm{s}})$ to account for the impact of user activity detection and assume that the channel gains are estimated perfectly after successful user activity detection. For the case of an erroneous user activity detection, the packet of user 1 cannot be decoded correctly. For the case of correct detection of user activity, the BS receiver is able to decode user 1's packet using multi-user detection, with a decoding error probability

$P_{\mathrm{err}}(N_{\mathrm{s}})$. Consequently, the packet drop probability for user 1 is calculated as

$$P_{\mathrm{drop}}(N_{\mathrm{cell}}) = \sum_{N_{\mathrm{s}}=0}^{N_{\mathrm{cell}}-1} P_{\mathrm{col}}(N_{\mathrm{s}}) P_{\mathrm{miss}}(N_{\mathrm{s}})$$
$$+ \sum_{N_{\mathrm{s}}=0}^{N_{\mathrm{cell}}-1} P_{\mathrm{col}}(N_{\mathrm{s}}) \left[1 - P_{\mathrm{miss}}(N_{\mathrm{s}})\right] P_{\mathrm{err}}(N_{\mathrm{s}}) . \tag{38}$$

C. Supported User Density and System Throughput

Given the packet drop probability from (38), we can define the supported user density as

$$\mathcal{D}_{\mathrm{cell}} \triangleq \max (N_{\mathrm{cell}}) \text{ such that } P_{\mathrm{drop}}(N_{\mathrm{cell}}) \leq \varepsilon \tag{39}$$

and the system throughput as

$$\mathcal{T}_{\mathrm{cell}} \triangleq \frac{N_{\mathrm{cell}} \lambda_{\mathrm{a}}}{K_{\mathrm{b}} \Delta f \Delta t} \left[1 - P_{\mathrm{drop}}(N_{\mathrm{cell}})\right] . \tag{40}$$

The user density in (39) is the maximum number of supported users per cell such that the packet drop probability does not exceed a given threshold $\varepsilon > 0$. The system throughput in (40) is the number of correctly decoded packets per second per Hz, where Δf is the bandwidth of the TFRB and Δt denotes the TTI.

D. Connection to WL Receivers

Now we determine $P_{\mathrm{err}}(N_{\mathrm{s}})$ as a function of the BS receiver type, using the expressions derived in Section III.

For the WL receivers, the decoding error probability is given by

$$P_{\mathrm{err}}(N_{\mathrm{s}}) = \begin{cases} \mathcal{P}_{\mathrm{WZF}}(N_{\mathrm{s}}+1) , & \text{for WL-ZF} \\ \mathcal{P}_{\mathrm{WMMSE}}(N_{\mathrm{s}}+1) , & \text{for WL-MMSE} \end{cases} \tag{41}$$

for $N_{\mathrm{s}} \leq 2M - 1$. For $N_{\mathrm{s}} \geq 2M$, there is at least one interference signal that cannot be suppressed by the WL-ZF and WL-MMSE receivers. In this case, the error probability can be well approximated as $P_{\mathrm{err}}(N_{\mathrm{s}}) = 1$ [1].

For the CL receivers, as the maximum number of suppressed interfering users is $N_{\mathrm{s}} = M - 1$, their decoding error probability is approximated by 1 for the case of $N_{\mathrm{s}} \geq M$. For the case of $N_{\mathrm{s}} \leq M - 1$, the decoding error probability is

$$P_{\mathrm{err}}(N_{\mathrm{s}}) = \begin{cases} \mathcal{P}_{\mathrm{CZF}}(N_{\mathrm{s}}+1) , & \text{for CL-ZF} \\ \mathcal{P}_{\mathrm{CMMSE}}(N_{\mathrm{s}}+1) , & \text{for CL-MMSE} \end{cases} , \tag{42}$$

where $\mathcal{P}_{\mathrm{CZF}}$ and $\mathcal{P}_{\mathrm{CMMSE}}$ denote the outage probability of the CL-ZF and CL-MMSE receivers, respectively, and can be derived from the complex-valued model (1), following steps similar to those for the WL-ZF and WL-MMSE receivers from Section III.

We observe that the WL receivers are able to resolve more colliding packets, thereby resulting in a lower packet drop probability than the CL receivers. Hence, for a given packet drop probability, one can expect that grant-free MTC systems can support higher user density and larger system throughput due to the use of WL receivers.
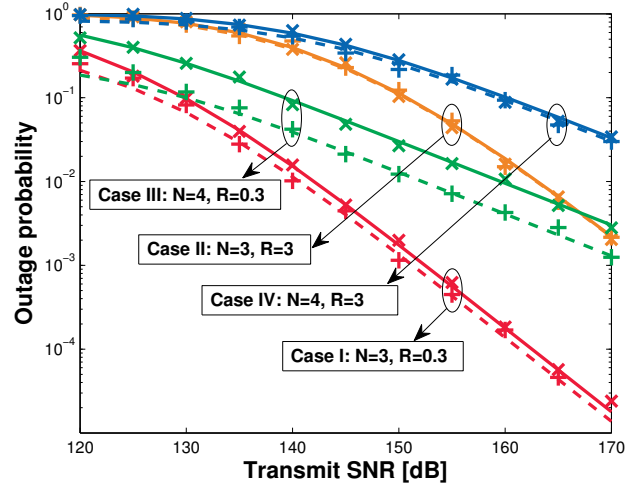

Fig. 1. Outage probability for WL-ZF and WL-MMSE receivers, where the simulated results are marked by '×' and '+' for ZF and MMSE respectively, and the analytical results are indicated by the solid line and dashed line for ZF and MMSE respectively. The number of receiver antennas is $M = 2$.

V. NUMERICAL RESULTS

In this section, we first validate the correctness of the outage performance analysis for WL receivers from Section III. We then evaluate the connectivity performance of grant-free MTC systems using WL receivers as presented in Section IV, for which we consider NB-IoT as a specific example system.

A. Receiver Performance Evaluation

In an NB-IoT system, the transmit power levels of users are adjusted through an open-loop process with pathloss compensation [26, Sec. 7.3.3.2.2]. Since NB-IoT is primarily used for coverage enhancement, the pathloss factor experienced by the devices is very high. This can also be true if the device is close to the base station, as it may be located indoors or in a basement. The transmitted signal will suffer from increased attenuation and therefore, the transmit power is often set to the maximum possible value to improve the coverage. Consequently, the impact of power control on the receiver performance is limited for the NB-IoT scenario considered. Hence, for the receiver performance evaluation, we consider the NPC case and generate the power variation term ϕ_i according to

$$\phi_i = \beta_i + \psi_i \text{ dB} . \tag{43}$$

The pathloss factor used for NB-IoT link-level evaluation [26, Annex D] is specified as $\beta_i = -120.9 - 37.6 \log_{10}(r_i)$ dB, $0 \leq r_i \leq r_{\mathrm{cell}}$, where r_i is the distance in kilometers between user i and the base station, and $r_{\mathrm{cell}} = 0.91$ km is the cell radius. The shadowing fading factor ψ_i in dB is specified as a Gaussian distributed random variable with zero mean and standard deviation 8 dB [26, Annex D]. All users are assumed to be uniformly distributed at random in the cell. The SNR gap between channel capacity and practical modulation and coding schemes is set to be $\Gamma = 6$ dB [33], for short-packet communications over 5G networks.
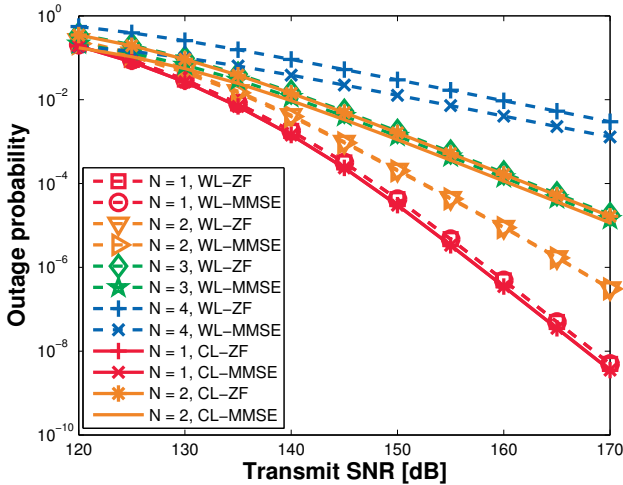
Fig. 2. Outage probability comparison between WL and CL receivers, where the number of receiver antennas is $M = 2$ and the target data rate is $R = 0.3$ bits/sec/Hz.

Fig. 1 shows the outage probability for WL-ZF and WL-MMSE receivers as a function of the transmitter SNR ρ (4), for $M = 2$ receiver antennas at the BS and four cases with different values for the number of users N and target rate R. We observe that in all cases, the simulated results match well with the analytical ones, and the WL-MMSE receivers have a lower outage probability than the corresponding WL-ZF receivers. Comparing Case I to Case II and Case III to Case IV, we see that the SNR gap between the outage probability curves of WL-ZF and WL-MMSE is smaller in the high rate scenario with $R = 3$ bits/sec/Hz, which coincides with our earlier analysis. Furthermore, comparing Case I to Case III and Case II to Case IV, we note that the SNR gain due to MMSE is more remarkable when there are more users to detect. This is because the additional term $\eta_{\mathrm{WL},n}$ in (25) has a larger DoF as N increases (see (34)) and can thus improve more the outage probability over that of the ZF receiver.

Fig. 2 compares the outage probabilities of WL and CL receivers in the dual-antenna case $M = 2$. When detecting only a single user, the WL and CL receivers have nearly the same decoding performance except a negligible SNR gap. The slight SNR loss of WL receivers is due to the fact that one-dimensional coding schemes cannot exploit the DoFs as efficiently as two-dimensional coding schemes [29]. When the number of users is increased by 1 for both the WL and CL receivers ($N_{\mathrm{WL}} = N_{\mathrm{CL}} = 2$), the WL receivers have a lower outage probability than the CL receivers due to a higher diversity order. Furthermore, we observe that the WL transmission with $N_{\mathrm{WL}} = 3$ users provides almost the same outage probability as the CL transmission with $N_{\mathrm{WL}} = 2$ users. These results demonstrate the benefits of the WL paradigm for MTC systems with a large number of devices.

TABLE I
NB-IoT SYSTEM PARAMETERS USED FOR SIMULATION

Parameter	Value
Area of one sector	0.86 km^2
Number of sectors per cell	3
IoT user deployment	Uniform distribution within a cell
Transmitter power (maximum)	23 dBm
Noise power spectral density	-174 dBm/Hz
Receiver noise figure	5 dB
System total bandwidth	180 kHz
Subcarrier spacing	3.75 kHz
Transmission time interval	32 ms
Transport block size	32 bits
Arrival time distribution	Poisson distribution
Packet arrival rate	1.3×10^{-4} packets/s/user

B. Connectivity Performance Evaluation

Having confirmed the accuracy of the outage performance analysis, we now turn to the user density and system throughput performance to assess the benefits of the WL paradigm to support mMTC. We apply the parameters typical for NB-IoT systems, which are obtained from [26] and summarized in Table I. Assuming that 10% of the duration of one TTI is used for preamble transmission, the target data rate is calculated as $R = \frac{32}{32 \cdot 10^{-3} \times 3750}/0.9 \approx 0.3$ bits/sec/Hz. NB-IoT with BPSK for WL detection would employ coding with a rate 1/3 to achieve this rate, while QPSK modulation and coding with a rate 1/6 is applicable for CL detection at the BS. The transmit SNR for all NB-IoT devices is set to be $\rho = 156.26$ dB, calculated from the maximum transmit power 23 dBm. For a required SNR of -7 dB at the BS [26], this corresponds to a maximum coupling loss (MCL) of about 164 dB, which is the desired operating regime for NB-IoT devices. The large-scale fading as in (43) and the SNR gap Γ (dB) $= 6$ dB are still applied. For the grant-free access protocol, we consider the single-tone transmission in NB-IoT systems and thus assume that each TFRB uses one subcarrier of 3.75 kHz. Hence the number of TFRBs is equal to the number of subcarriers, calculated as $K_{\mathrm{b}} = 48$. The packet arrival rate is converted to $\lambda_{\mathrm{a}} = 4.16 \times 10^{-6}$ packets/TTI/user, which is a typical value for NB-IoT traffic [26]. Finally, we assume that the user activity detection is not the bottleneck of the system performance and hence apply[5] $P_{\mathrm{miss}}(N_{\mathrm{s}}) = 10^{-2} P_{\mathrm{err}}(N_{\mathrm{s}})$ so as to focus on the effect of WL detection on overall performance.

Fig. 3 compares the packet drop probabilities for the WL and CL schemes as a function of user density. According to [26], a packet drop probability $\varepsilon \leq 1\%$ is desirable for NB-IoT. We observe that at around $\varepsilon = 1\%$, the supported number of users increases from 50k to 500k due to WL reception at a single-antenna BS, i.e., the user density can be increased by 10 times. For the dual-antenna BS case, an improvement by a factor of 6, from about 500k to 3000k users per cell

---

[5]In general, the missed detection probability need not have an explicit relationship with the probability of error in packet decoding. However, for system modelling, it is typically taken to be two orders of magnitude lower than the probability of error in packet decoding [34]. Otherwise, it becomes a bottleneck for system performance. Therefore, using $P_{\mathrm{miss}}(N_{\mathrm{s}}) = 10^{-2} P_{\mathrm{err}}(N_{\mathrm{s}})$, we exclude the impact of user activity detection and focus on the performance gains from WL reception.
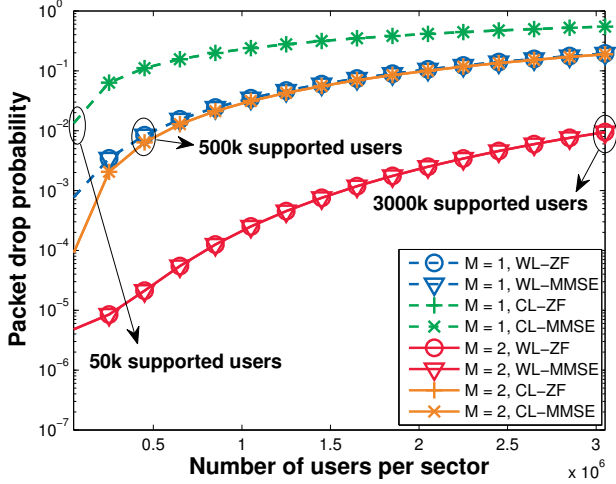
Fig. 3. Packet drop probability comparison between WL and CL receivers in uplink grant-free NB-IoT systems.

Fig. 5. Collision probability $P_{col}(N_s)$ versus the number of colliding users N_s, where "N_s colliding users" means that there are total $N_s + 1$ users transmitting a packet over the same TFRB.
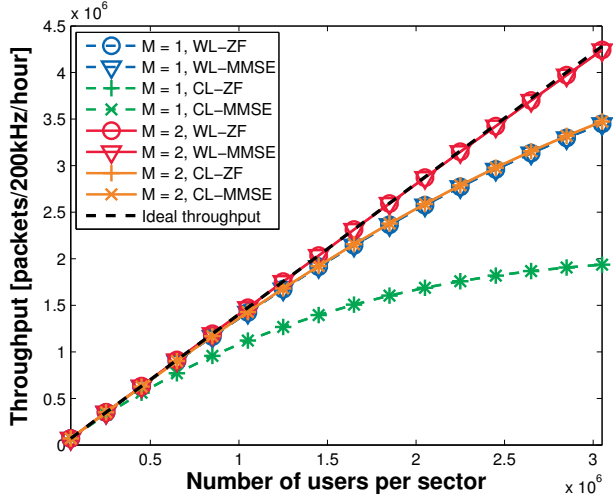

Fig. 4. System throughput comparison between WL and CL receivers in uplink grant-free NB-IoT systems.

sector, is achieved. Also, it should be noted that the packet drop probability curves of ZF and MMSE receivers coincide, because the ZF and MMSE receivers have nearly the same outage performance in Fig. 2. Although an outage probability difference can be seen for WL-ZF and WL-MMSE receivers in the case of $N = 4$, it has a minor impact on the overall packet drop probability, since the cases of $N = 1, 2, 3$ are dominating, as will be shown in Fig. 5.

The throughputs for the WL and CL schemes are compared in Fig. 4. The dashed line corresponds to the ideal case that every packet is decoded correctly, and it is included as a reference. It can be seen that the WL receiver can significantly improve the system throughput in both the single-antenna and dual-antenna cases. Furthermore, for the dual-antenna case, the WL receiver provides nearly an ideal throughput for a large range of user densities. From Figs. 3 and 4, we note that the WL receivers with only a single antenna have nearly the
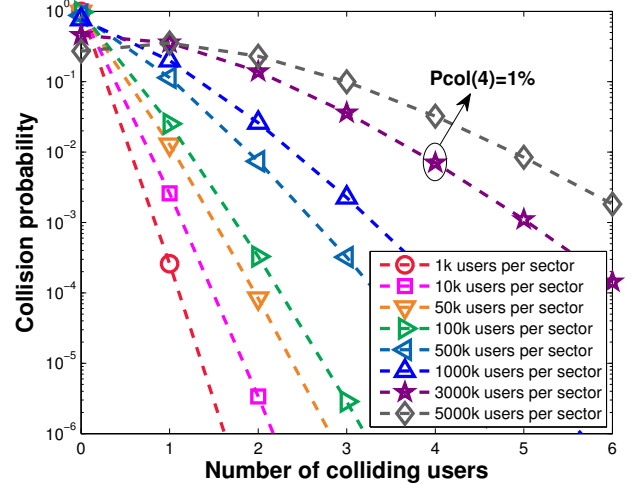
same packet drop probability and system throughput as the CL receivers with two antennas. Hence, in terms of system-level performance, the use of WL processing virtually doubles the number of receive antennas.

We furthermore observe from Figs. 3 and 4 that ZF and MMSE receivers yield nearly the same packet drop probability and thus identical system throughput. This is because of the low outage probability at around $\rho = 156$ dB (see Fig. 2), which means that the packet drop probability is mainly determined by the collision probability.

To further clarify this, the collision probability as a function of user density is shown in Fig. 5. For example, the dual-antenna WL receivers are able to resolve $N_s = 3$ colliding packets and thus the corresponding packet drop probability is mainly determined by the collision probability for $N_s = 4$. We have $P_{col}(4) \approx 1\%$ when the user density is increased to 3000k users/sector, which is consistent with the result in Fig. 3 at $\varepsilon \approx 1\%$. Similarly, (i) $P_{col}(1) \approx 1\%$ for 50k users and (ii) $P_{col}(2) \approx 1\%$ at about 500k users, which correspond to the 1% packet drop probability results for (i) CL single-antenna and (ii) CL dual-antenna and WL single-antenna receivers in Fig. 3, respectively. Hence, we conclude that the improvement of supported user density is mainly due to the superior user-multiplexing capability of WL receivers.

Finally, Fig. 6 shows the supported user density as a function of the number of users per cell sector using the simplifications

$$ P_{err}(N_s) = \begin{cases} 0, & 0 \le N_s \le c \cdot M - 1 \\ 1, & N_s > c \cdot M - 1 \end{cases}, \quad (44) $$

where $c = 1$ for the CL and $c = 2$ for the WL case, and $P_{miss} = 0$ in (38) and a target drop rate of $\varepsilon = 1\%$. We observe that the improvement in user density decreases as the number of receiver antennas M increases. This is because the user-overloading probability for CL receivers, i.e., the probability of $N_s > M$, decreases as M increases. Hence, the use of WL receivers, which can resolve collisions up to $N_s \le 2M$,
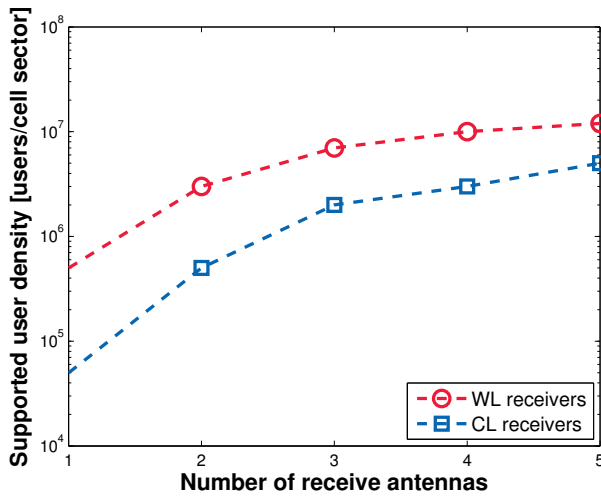
Fig. 6. Supported user density for WL and CL receivers in uplink grant-free NB-IoT systems considering a packet drop rate of 1% as a function of the number of receive antennas M.

is expected to yield a less pronounced benefit for larger M. Nevertheless, the gain in supported user density due to the use of WL processing is still substantial in the multi-antenna cases.

VI. Conclusions

Considering the demand for massive connectivity driven by the proliferation of various IoT applications, we have investigated the use of real-valued transmission together with WL receivers to the uplink of grant-free MTC systems. The outage probability of WL receivers has been analyzed to demonstrate their advantage over the CL counterparts in terms of user multiplexing and transmission reliability. The improved user multiplexing for WL receivers has been shown to be the key for enhancing the connectivity performance of current grant-free MTC systems. For the specific example of NB-IoT system, we have shown that the supported user density and system throughput can be significantly increased due to the use of WL receivers. We note that the WL paradigm can be combined with other schemes such as, e.g., NOMA, suitable for mMTC systems serving IoT applications. The application of WL paradigm to such schemes will be an interesting direction of work for the future.

References

[1] R. Gui, N. M. Balasubramanya, G. Prasad, and L. Lampe, "Uplink performance analysis for grant-free narrowband IoT with widely linear receiver," in *IEEE Global Communications Conference (Globecom)*, 2019, pp. 1–6.

[2] Z. Dawy, W. Saad, A. Ghosh, J. Andrews, and E. Yaacoub, "Toward massive machine type cellular communications," *IEEE Wireless Commun.*, vol. 24, no. 1, pp. 120–128, 2017.

[3] S. Mumtaz, A. Alsohaily, Z. Pang, A. Rayes, K. F. Tsang, and J. Rodriguez, "Massive internet of things for industrial applications: Addressing wireless IIoT connectivity challenges and ecosystem fragmentation," *IEEE Ind. Electron. Mag.*, vol. 11, no. 1, pp. 28–33, 2017.

[4] C. Bockelmann, N. Pratas, H. Nikopour, K. Au, T. Svensson, C. Stefanovic, P. Popovski, and A. Dekorsy, "Massive machine-type communications in 5G: Physical and MAC-layer solutions," *IEEE Commun. Mag.*, vol. 54, no. 9, pp. 59–65, 2016.

[5] Y. E. Wang, X. Lin, A. Adhikary, A. Grovlen, Y. Sui, Y. Blankenship, J. Bergman, and H. S. Razaghi, "A primer on 3GPP narrowband internet of things," *IEEE Commun. Mag.*, vol. 55, no. 3, pp. 117–123, Mar. 2017.

[6] J. Xu, J. Yao, L. Wang, Z. Ming, K. Wu, and L. Chen, "Narrowband internet of things: Evolutions, technologies, and open issues," *IEEE Internet Things J.*, vol. 5, no. 3, pp. 1449–1462, Jun. 2018.

[7] G. Berardinelli, N. H. Mahmood, R. Abreu, T. Jacobsen, K. Pedersen, I. Z. Kovács, and P. Mogensen, "Reliability analysis of uplink grant-free transmission over shared resources," *IEEE Access*, vol. 6, pp. 23 602–23 611, 2018.

[8] Z. Ding, X. Lei, G. K. Karagiannidis, R. Schober, J. Yuan, and V. K. Bhargava, "A survey on non-orthogonal multiple access for 5G networks: Research challenges and future trends," *IEEE J. Sel. Areas Commun.*, vol. 35, pp. 2181–2195, 2017.

[9] L. Liu and W. Yu, "Massive connectivity with massive MIMO—Part I: Device activity detection and channel estimation," *IEEE Trans. Signal Process.*, vol. 66, no. 11, pp. 2933–2946, 2018.

[10] A. Bayesteh, E. Yi, H. Nikopour, and H. Baligh, "Blind detection of SCMA for uplink grant-free multiple-access," in *International Symposium on Wireless Communications Systems (ISWCS)*, 2014, pp. 853–857.

[11] M. Mohammadkarimi, M. A. Raza, and O. A. Dobre, "Signature-based nonorthogonal massive multiple access for future wireless networks: Uplink massive connectivity for machine-type communications," *IEEE Veh. Technol. Mag.*, vol. 13, no. 4, pp. 40–50, 2018.

[12] B. Picinbono and P. Chevalier, "Widely linear estimation with complex data," *IEEE Trans. Signal Process.*, vol. 43, no. 8, pp. 2030–2033, Aug. 1995.

[13] A. Lampe and M. Breiling, "Asymptotic analysis of widely linear MMSE multiuser detection-complex vs real modulation," in *IEEE Information Theory Workshop*, 2001, pp. 55–57.

[14] R. Meyer, W. H. Gerstacker, R. Schober, and J. B. Huber, "A single antenna interference cancellation algorithm for increased GSM capacity," *IEEE Trans. Wireless Commun.*, vol. 5, no. 7, pp. 1616–1621, 2006.

[15] P. Chevalier and F. Pipon, "New insights into optimal widely linear array receivers for the demodulation of BPSK, MSK, and GMSK signals corrupted by noncircular interferences-application to SAIC," *IEEE Trans. Signal Process.*, vol. 54, no. 3, pp. 870–883, 2006.

[16] R. Schober, W. H. Gerstacker, and L. Lampe, "Data-aided and blind stochastic gradient algorithms for widely linear MMSE MAI suppression for DS-CDMA," *IEEE Trans. Signal Process.*, vol. 52, no. 3, pp. 746–756, 2004.

[17] J. G. Proakis and M. Salehi, *Digital Communications*. McGraw-hill New York, 2001, vol. 4.

[18] T. Adali, P. Schreier, and L. Scharf, "Complex-valued signal processing: The proper way to deal with impropriety," *IEEE Trans. Signal Process.*, vol. 59, no. 11, pp. 5101–5125, Nov. 2011.

[19] S. Buzzi, M. Lops, and S. Sardellitti, "Widely linear reception strategies for layered space-time wireless communications," *IEEE Trans. Signal Process.*, vol. 54, no. 6, pp. 2252–2262, 2006.

[20] K. Kuchi and V. K. Prabhu, "Performance evaluation for widely linear demodulation of PAM/QAM signals in the presence of Rayleigh fading and co-channel interference," *IEEE Trans. Commun.*, vol. 57, no. 1, pp. 183–193, 2009.

[21] D. Korpi, L. Anttila, V. Syrjälä, and M. Valkama, "Widely linear digital self-interference cancellation in direct-conversion full-duplex transceiver," *IEEE J. Sel. Areas Commun.*, vol. 32, no. 9, pp. 1674–1687, 2014.

[22] "Study on network-assisted interference cancellation and suppression (NAIC) for LTE," 3GPP, Tech. Rep. 36.866 v. 12.0.1, Mar. 2014.

[23] "Comparison of pi/2 BPSK with and without frequency domain pulse shaping: Results with PA model," 3GPP R1-1701180, Tech. Rep., Jan. 2017.

[24] *Evolved Universal Terrestrial Radio Access (E-UTRA); LTE Physical layer; General description*, 3GPP Std. 36.201 v. 14.1.0, Apr. 2017.

[25] *Evolved Universal Terrestrial Radio Access (E-UTRA) and Evolved Universal Terrestrial Radio Access Network (E-UTRAN); Physical Channels and Modulation*, 3GPP Std. 36.211 v. 13.3.0, Sep. 2017.

[26] "Cellular system support for ultra low complexity and low throughput internet of things," 3GPP, Tech. Rep. 45.820 v. 13.1.0, Aug. 2015.

[27] C. Bockelmann, N. K. Pratas, G. Wunder, S. Saur, M. Navarro, D. Gregoratti, and G. Vivier, "Towards massive connectivity support for scalable mMTC communications in 5G networks," *IEEE Access*, vol. 6, pp. 28 969–28 992, 2018.

[28] Y. Jiang, M. K. Varanasi, and J. Li, "Performance analysis of ZF and MMSE equalizers for MIMO systems: An in-depth study of the high SNR regime," *IEEE Trans. Inf. Theory*, vol. 57, pp. 2008–2026, 2011.

[29] D. Tse and P. Viswanath, *Fundamentals of Wireless Communication*. Cambridge University Press, 2005.

[30] N. Shariati, E. Björnson, M. Bengtsson, and M. Debbah, "Low-complexity polynomial channel estimation in large-scale MIMO with arbitrary statistics," *IEEE J. Sel. Areas Commun.*, vol. 8, no. 5, pp. 815–830, 2014.

[31] X.-D. Zhang, *Matrix Analysis and Applications*. Cambridge University Press, 2017.

[32] K. P. Murphy, *Machine Learning: A Probabilistic Perspective*. MIT Press, 2012.

[33] A. Azari, P. Popovski, G. Miao, and C. Stefanovic, "Grant-free radio access for short-packet communications over 5G networks," in *IEEE Global Communications Conference (Globecom)*, 2017, pp. 1–7.

[34] C. Wang, Y. Chen, Y. Wu, and L. Zhang, "Performance evaluation of grant-free transmission for uplink URLLC services," in *Vehicular Technology Conference (VTC Spring)*, 2017, pp. 1–6.

Ronghua Gui received the B.Eng. and Ph.D. degrees in information and communication engineering from the University of Electronic Science and Technology of China (UESTC), Chengdu, China, in 2015 and 2020, respectively. From 2018 to 2019, he was a visiting student at the University of British Columbia (UBC), Vancouver, working on the detection technology for massive machine-type communications (mMTC). His research interests focus on array signal processing with its applications in radar systems and wireless communications.

Naveen Mysore Balasubramanya received the M.S. degree in electrical engineering from the University of Colorado, Boulder, USA, in 2010 and the Ph.D. degree in Electrical and Computer Engineering from The University of British Columbia, Vancouver, BC, Canada in 2017. Since September 2018, he has been an Assistant Professor at the Indian Institute of Technology Dharwad, Karnataka, India. He has a rich academic experience as well as six years of industrial R&D experience, having worked as a postdoctoral research associate at Heriot-Watt University, Edinburgh, U.K. and as a Senior Design Engineer for the ADSL, WiMAX, and LTE Systems in leading communication industries, such as, Lantiq Communications (Intel) India Pvt. Ltd., Broadcom Communications India Pvt. Ltd., and Tata Elxsi Ltd., Bangalore, India. His research interests are broadly in theory and practical aspects of wireless communications, with focus on next generation communication technologies and energy efficient Internet of Things.
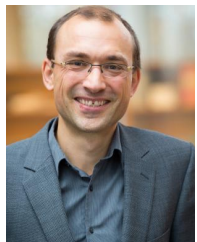
Lutz Lampe (M'02-SM'08) received the Dipl.-Ing. and Dr.-Ing. degrees in electrical engineering from the University of Erlangen, Erlangen, Germany, in 1998 and 2002, respectively. Since 2003, he has been with the Department of Electrical and Computer Engineering, The University of British Columbia, Vancouver, BC, Canada, where he is a Full Professor. His research interests are broadly in theory and application of wireless, optical wireless, optical fiber, power line and underwater acoustic communications. He has served as an Associate Editor and a Guest Editor for several IEEE journals, and as a General and Technical Program Committee Co-Chair for IEEE conferences. He has been a Distinguished Lecturer of the IEEE Communications Society and a (co-)recipient of a number of best paper awards. He is a co-editor of the book "Power Line Communications: Principles, Standards and Applications from Multimedia to Smart Grid" (2nd ed.) by John Wiley & Sons.